A FIRST CONSISTENT ANALYSIS OF EROSION OF THE ITER VERTICAL TARGETS FOR DISRUPTIONS AND ELMs

H. Würz, S. Pestchanyi* and F. Kappler

Forschungszentrum Karlsruhe, INR, Postfach 36 40, D-76021 Karlsruhe
**Troitsk Institute for Innovation and Fusion Research, 142092 Troitsk, Russia*

1. Introduction

As is well known a plasma shield from vaporized target material formed in front of the divertor during plasma disruptions reduces the target heat load because it converts the energy of the hot plasma into hydrodynamic motion, ionization and radiation of the plasma shield [1]. A realistic quantification of erosion of the ITER slot divertor needs a 2D analysis because of the finite width of the disruptive SOL plasma, the unsymmetrical distribution of power density across the SOL plasma, because of the tilting of the target and the subsequent complicated MHD behaviour of the plasma shield [2] and because of possible damages of the divertor wings by radiation emitted from the intensely radiating plasma shield in front of the in- and outboard targets [3]. Therefore the 2D radiation magnetohydrodynamics (R-MHD) code FOREV-2 was developed [4].

This paper discusses the validation of FOREV-2 against results from hot plasma target experiments performed at the plasma gun facilities 2MK-200 CUSP [5] and MK-200 CUSP [6] at TRINITI Troitsk. Moreover the results of an analysis of MHD motion of plasma shields and erosion of ITER vertical targets are presented.

2. Energy balance in disruptive hot plasma target interactions

For power densities of the hot SOL plasma below 44 MW/cm^2 along the magnetic field lines (4 MW/cm^2 to a horizontal target and about 1.2 MW/cm^2 to a vertical target) heat deposition by the impacting hot plasma dominates the target heat at all times as is shown in Fig. la for a horizontal graphite target and a target power density of 1 MW/cm^2. The disruptive hot plasma is assumed to consist from 10 keV ions and 10 keV Maxwellian electrons with equal energy carried by ions and electrons. According to Fig. 1a, there is agreement of results on evolution of heat deposition by the impacting hot plasma and by radiation from 1 dim calculations with FOREV-1 [7] and from 2 dim calculations with FOREV-2. Electron heat conduction only plays a role as target heat source at early times. At later times the plasma temperature profile in the plasma shield close to the target becomes constant in a layer of thickness of 0.4 mm thus blocking the heat transfer by electron heat conduction.

The energy laterally radiated away from the plasma shield amounts up to 85 % of the input energy. With ongoing time as seen from Fig. 1b it is deposited along the side wall of the slot divertor over a distance of up to 2 m from the target. Side walls from Be opposite to a vertical target and at a distance of 30 cm would melt after 0.8 ms. After 10 ms the melt layer thickness would be about 100 μm. For tungsten and times up to 10 ms the surface temperature remains below 2000 K. For power densities of the hot plasma below 1 MW/cm^2 melting of tungsten side walls does not occur at any time, melting of Be occurs. As melt splashing can't be excluded, Be can't be used as divertor material. For a power density of 10 MW/cm^2, radiation dominates the target heat load after 200 μs. Energy deposition from the hot plasma

to the target stops after 450 μs. The radiation flux scales with the incoming power density. In this case, melting and vaporization occurs for all types of side wall materials. After 1 ms tungsten and after 0.2 ms Be start to melt over the full length of the slot extension.

3. Validation of FOREV-2

At TRINITI Troitsk, hot plasma target experiments were performed at the plasma gun facilities 2MK-200 CUSP [5] and MK-200 CUSP [6]. The hot plasma β value was below 0.3, the hot plasma ion temperature was around 500 eV, the Maxwellian distributed hot electrons had temperatures of around 300 eV. Experiments were performed with perpendicular targets. In this case, the magnetic field lines are perpendicular to the target, thus simulating a horizontal target in the poloidal plane but neglecting the toroidal component of the magnetic field. The power density profile of the impacting hot plasma was assumed to be Gaussian with a half width of 0.5 cm and its time evolution to have a half width of 10 μs. Peak power density is reached after 3 μs, remains constant for 5 μs and then decays exponentially. Calculated and measured electron temperature profiles in the center of the plasma shield at 10 μs are shown in Fig. 2 for an energy density of the hot plasma of 200 J/cm^2. At a distance of 1 cm from the target, the temperature is up to 50 eV whereas in the tokamak plasma shield it is only 1 eV. Due to this steep temperature gradient, electron heat conduction becomes the dominating target heat source in these experiments. Direct energy deposition of the hot plasma to the target is negligible. Because of the low impact energy, the hot plasma after 0.8 μs is fully stopped in the plasma shield.

Calculated and measured electron density profiles at different distances from the target and for different times are shown in Figs. 3 for a peak power density of the hot plasma of 42 MW/cm^2. Lateral plasma jets are observed at larger distances. The calculated profiles and density values are in a rather good agreement with the measured values. The reason for the lateral jets is momentum transfer from the hot plasma ions. Lateral jets are not occurring at peak power densities of 20 MW/cm^2. The flow pattern closer to the target is the same for both power densities. At early times the plasma flows across the magnetic field lines to the center (inward flow) as seen from Fig. 4 which shows 2D electron density contours and the flow pattern. The thickness of the layer in which this flow occurs is about 1.5 mm. The reason for the inward flow is pushing away of the guiding magnetic field component B_x at the center by the plasma shield. Due to its high electric conductivity the magnetic field lines are frozen in at the graphite target. Then a y-component of magnetic field arises causing the inward plasma flow. Later in time, the pushing out of B_x decreases and only momentum transfer by the hot ions continues. As a consequence, the plasma flow close to the target changes its direction and flows outward. The target heat flux by electron heat conduction is shown in Fig. 5. Caused by preferential inward movement it drops at around 15 μs and again contributes after flow reversal. The calculated erosion is 0.25 μm, the measured value is 0.2 μm.

Comparison of results was also done for quartz. Quartz has a smaller electric conductivity and therefore B_x is not frozen in at the target. Pushing out of B_x by the vaporized material now occurs also at the target. Consequently the plasma shield is experiencing only a weak lateral magnetic force and momentum transfer from the hot plasma ions is dominating the movement. As a consequence, the plasma close to the target flows along the target in outward direction. This outward flow just from the beginning reduces the plasma shield

density at the center, increases the plasma temperature and thus results for at least 10 μs in a higher electron heat conduction flux to the target in comparison with graphite as shown in Fig. 5. Typically, this target heat flux amounts up to 1 MW/cm^2, whereas the radiative heat flux is around 0.02 MW/cm^2. Fig. 6 shows a comparison of measured and calculated time dependence of erosion for quartz at two different positions. The calculated erosion values are in good agreement with the measured ones. In the experiment, the time dependent erosion left and right from the center differs because of the asymmetric power density profile of the hot plasma [1]. In the calculation, a Gaussian profile was used.

4. MHD motion of plasma shields and erosion of vertical targets

The tilting angle of the vertical target in the poloidal plane was assumed to be 20^o. Realistic unsymmetrical power density profiles across the SOL with peak target heat fluxes of 0.3 MW/cm^2 and with separatrix up- and downstream were used [2]. 2 dim plasma density profiles and the plasma flow pattern (arrows) in the plasma shield are shown in Fig. 7a for the upstream and the downstream separatrix strike point at 600 μs for a peak target heat flux of 0.3 MW/cm^2. The density lines correspond to carbon densities in the range of 4×10^{16} to 5×10^{17} cm^{-3}. In case of upstream separatrix strike point, the downward flow results in a depletion of shielding at the position of the strike point, whereas in case of downstream separatrix strike point the downward flow results in an improved shielding at the strike point position. From Fig. 7b it is seen that the erosion profiles are markedly different for both cases. For the downstream separatrix strike point peak erosion is about a factor of 10 less than for the case with upstream strike point. The plasma fans seen in Fig. 7a in front of the upper side wall in both cases are target plasma which outside of the hot plasma impact region flow upstream (in x-direction) with velocities typically of $3 \times l0^5$ cm/s. Again, this flow pattern is caused by pushing out of B_x at the position of the separatrix. B_x decreases to 0.4 T. Both plasma fans have plasma temperatures of around 1 eV. They are weakly heated by lateral radiation fluxes of up to 0.03 MW/cm^2 from the central plasma shield.

5. Conclusions

In this report consistent 2D results based on a 2½D MHD model combined with 2D radiation transport are presented. Results from disruption simulation experiments hitherto not understood [1] now for the first time are interpreted and are fully reproduced by the 2D modeling. The MHD movement of the plasma shield and its importance for erosion was clearly demonstrated and the nature of the MHD flow across magnetic field lines was clarified. The 2D results obtained clearly demonstrate that a realistic analysis of disruptive erosion has to be performed with a 2D code.

References

[1] H. Würz et al.: Fusion Technology Vol. 32, No. 1, 1997, p. 45 - 74.
[2] S. Pestchanyi et al.: *24th EPS Conf. on Controlled Fusion and Plasma Physics*, Berchtesgaden, June 9 - 13, 1997, Vol. 21A, part III, p. 981.
[3] H. Würz et al.: Fusion Technology, Vol. 30, No. 3, 1996, p. 739.
[4] H. Würz et al.: Fusion Technology 1996, Vol. 1, p. 191, 1997.
[S] N.I. Arkhipov et al.: Fusion Technology 1994, Vol. 1, p. 463, 1995.
[6] N.I. Arkhipov et al.: J. Nucl. Mater **233 - 237** (1996) 767.
[7] B. Bazylev et al.: *22nd EPS Conf. on Controlled Fusion and Plasma Physics*, Bournemouth, July 3 - 7, 1995, Vol. 19C, part II, p. 277.

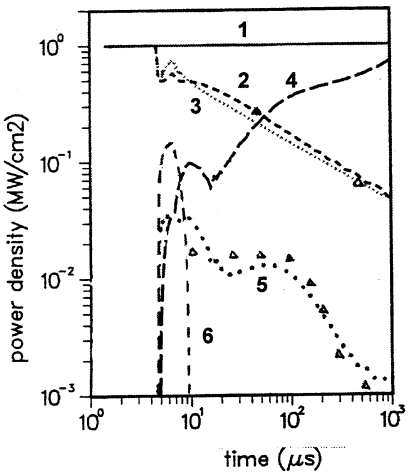

1 – power density of the hot plasma
2 – target heating by hot plasma
3 – heat flux into the target
4 – total lateral radiation
5 – radiation flux onto target
6 – electron heat conduction flux
Δ – results from FOREV2

Fig.1a. Time evolution of target heat fluxes for graphite target. Peak power density is 1 MW/cm². Results from FOREV-1 and FOREV-2.

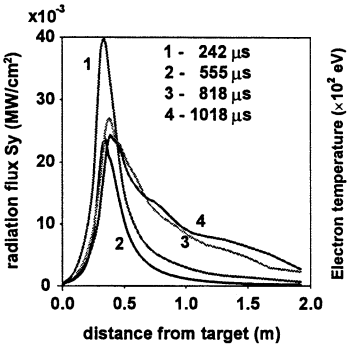

Fig.1b. Radiation flux to side wall. Peak power density is 1 MW/cm².

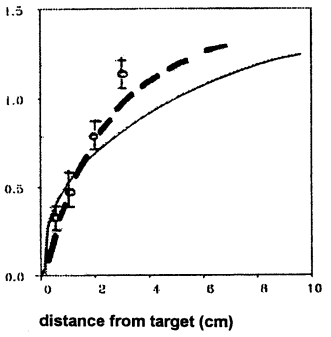

Fig.2. Comparison of measured and calculated electron temperature profiles in a carbon plasma shield. Peak power density is 18 MW/cm².

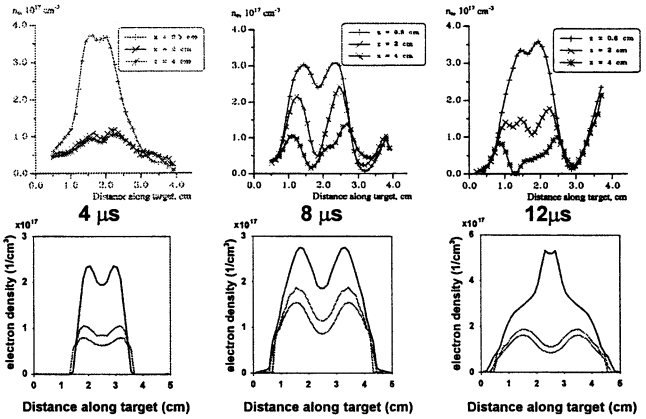

Fig.3. Comparison of calculated (above) and measured (below) electron density in a carbon plasma shield at different locations and times. Peak power density is 42 MW/cm².

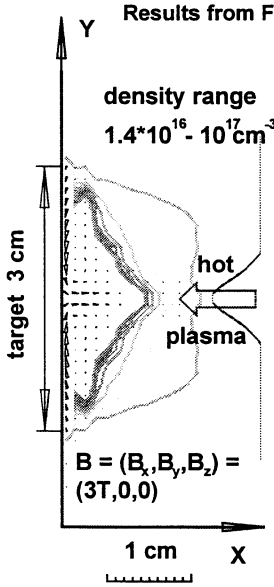

Fig.4. 2D electron density contours and flow pattern for graphite at 14 μs. Gaussian power density profile with peak value 20 MW/cm².

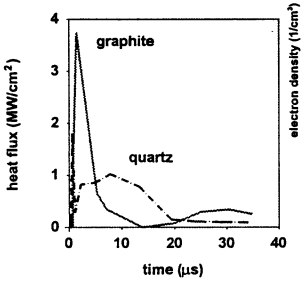

Fig.5. Comparison of electron heat conduction fluxes for graphite and quartz. Gaussian power density profile with peak value 20 MW/cm².

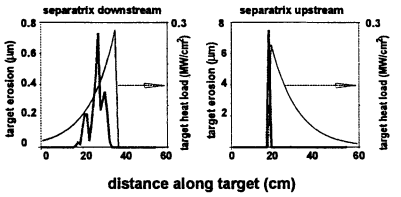

Fig.7b. Erosion and power density profiles along the inclined target at 1 ms.

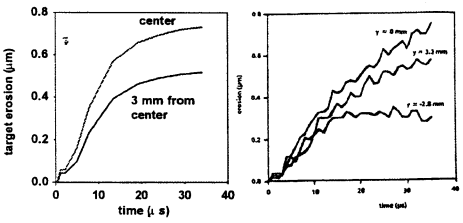

Fig.6. Comparison of measured and calculated time dependent erosion at different target positions.

Fig.7a. 2D plasma density contours and plasma flow pattern (arrows) in the plasma shield at 600 μs. Peak target heat load is 0.3 MW/cm².